

ELECTROCHEMICAL FABRICATION OF Mn₂O₃/MPC COMPOSITE FILM ELECTRODE AND ITS CHARACTERISTICS FOR HIGH-PERFORMANCE SUPERCAPACITORS

Mahanim Sarif @ Mohd Ali^{1,3}, *Zulkarnain Zainal^{1,2*}, Mohd Zobir Hussein¹, Mohd Haniff Wahid², Noor Nazihah Bahrudin² and Asla Abdullah Meed Al-Zahrani^{2,4}

¹*Materials Synthesis and Characterization Laboratory,
Institute of Advanced Technology, Universiti Putra Malaysia,
43400 UPM Serdang, Selangor, Malaysia*

²*Department of Chemistry, Faculty of Science, Universiti Putra Malaysia,
43400 UPM Serdang, Selangor, Malaysia*

³*Forest Product Division, Forest Research Institute Malaysia,
52109 Kepong, Selangor, Malaysia*

⁴*Imam Abdulrahman bin Fiasal University, Eastern Region, Dammam, Saudi Arabia.*

*Correspondence: zulkar@upm.edu.my

ABSTRACT

A composite film consisting of metal oxide (Mn₂O₃) and mesoporous carbon (MPC) was synthesised using the self-assembled spin coating soft templating method and incipient wetness of impregnation. The Mn₂O₃/MPC composite was characterised by Fourier transform infrared (FTIR), X-ray diffraction (XRD) and field emission scanning electron microscopy (FESEM). The electrochemical performance of synthesised composites in an electrolyte of 1 M potassium chloride (KCl) was evaluated by cyclic voltammetry (CV) and galvanostatic measurement of charge-discharge (GCD) and impedance analysis (EIS). Because of the pseudocapacitance of the dispersed Mn₂O₃ particles on the MPC surface, all composites with different Mn salt content showed higher specific capacitance than the pure MPC. The specific capacitance of the composite electrode when 10 wt% Mn salt was coated on the surface of MPC could reach 53.59 mF cm⁻². The R_{ct} value for the optimum composite film Mn₂O₃/MPC-10 wt% was 0.3 Ω lower than the MPC's carbon transfer resistance. The results showed that Mn₂O₃ can be used effectively in the electrode with the aid of MPC film components. This composite is very promising for the next generation of high-performance electrochemical supercapacitors.

Keywords: supercapacitor; pseudocapacitor; manganese oxide; mesoporous carbon

INTRODUCTION

An effective energy storage system has been greatly pursued in recent years due to the existence of many types of electrical and electronic devices. Supercapacitors are considered one of the most encouraging energy storage systems in the coming years due to its higher power density, faster charging and longer life cycle over lithium ion batteries [1]. Supercapacitors operate either by ion adsorption at the electrode/electrolyte interface of electrical double layer capacitors (EDLC) or rapid and reversible redox reactions in electrode materials (pseudocapacitors) [2-3]. The commonly used materials for the supercapacitor electrode are metal oxides due to their higher energy density than the carbon materials [1],[4] namely RuO₂ [5] and NiO [6], Co₃O₄ [7] or Fe₃O₄ [8]. Among all the metal oxides, manganese oxides (MnO, MnO₂, Mn₂O₃ and Mn₃O₄) offer advantages such as high specific capacitance (1233 F g⁻¹ for MnO₂), different oxidation states and crystallinity, low in cost and highly abundance, making it a promising electrode material for supercapacitors [9-10]. MnO_x's capacitance depends on the porosity, morphology, cation distribution, oxidation and crystal structure of the materials [10]. The high capacitance can be achieved by ultrathin MnO₂ films as the nanostructured materials can potentially access the storage sites throughout the MnO_x. Thus, the nanostructured MnO_x that can be accurately controlled and tailored for effective supercapacitor applications. For instance, the MnO_x electrode in supercapacitors undergoes redox reactions either by intercalating a charge carrier cation in the material gaps by the van der Waals force or chemisorptions on the surface [11].

In most cases, metal oxide's pseudocapacitive properties are often hybridized with carbon or organic materials as composites to improve the specific capacitance and the electrochemical performance [1],[2],[4],[11-15]. In the design of supercapacitor electrodes, a nanosized and high capacitance of MnO_x composite electrode incorporated with a highly conductive carbon material support would be advantageous. MnO₂/carbon aerogel [16], Mn₂O₃/mesoporous carbon [17-20], MnO₂/carbon nanotube, RuO₂/carbon nanotube and NiO/carbon nanotube [21] have been used for the production of composite electrode materials in recent years. The composites show an improved capacitive behaviour than their carbon counterparts due to their enhanced charge storage mechanisms with double layer capacitance [4],[12].

In this work, Mn salt was impregnated with an incipient wetness impregnation on MPC film at different concentrations (0 – 15 wt%) and calcined at 300 °C for 2 hours under nitrogen (N₂) gas flow to obtain the Mn₂O₃/MPC composite film. The prepared composites were used as electrodes for supercapacitors application and their respective electrochemical performance was examined.

EXPERIMENTAL

Materials

All materials and chemical reagents were analytically graded and obtained commercially from Chemolab Supplies Sdn Bhd and used directly without

pretreatment. Resorcinol (R) and triblock copolymer Pluronic F127 (F127) were obtained from Sigma Aldrich and Sigma respectively, while hydrochloric acid (HCl), manganese (II) acetate tetrahydrate $(\text{CH}_3\text{COO})_2\text{Mn}\cdot 4\text{H}_2\text{O}$ and ethanol were obtained from Merck whereas formaldehyde (F) were provided by Friendemann Schmidt. To prepare the solutions, deionized (DI) water of 18.2 Ω cm was used.

Preparation of $\text{Mn}_2\text{O}_3/\text{MPC}$ composites film

MPC carbon films were synthesized by polymerization of R and F with F127 as a pore forming agent and a catalyst of HCl [22]. Prior to the incorporation of metal oxide by the incipient wetness impregnation method, the optimized carbon film MPC was prepared. The composite film $\text{Mn}_2\text{O}_3/\text{MPC}$ was typically prepared as follows: A quantity of 10 wt % manganese (II) acetate tetrahydrate was dissolved in DI water and the titanium (Ti) foil was impregnated at room temperature for 150 min in the solution so that $(\text{CH}_3\text{COO})_2\text{Mn}\cdot 4\text{H}_2\text{O}$ would completely adsorb on the carbon surface of MPC. The quantity of Mn_2O_3 was set at 0, 5, 10 and 15 wt%, respectively. The resulting mixtures were dried for 12 hours at 80 °C and then calcined at 300 °C for 2 hours in the nitrogen atmosphere.

Characterization of structure and morphology

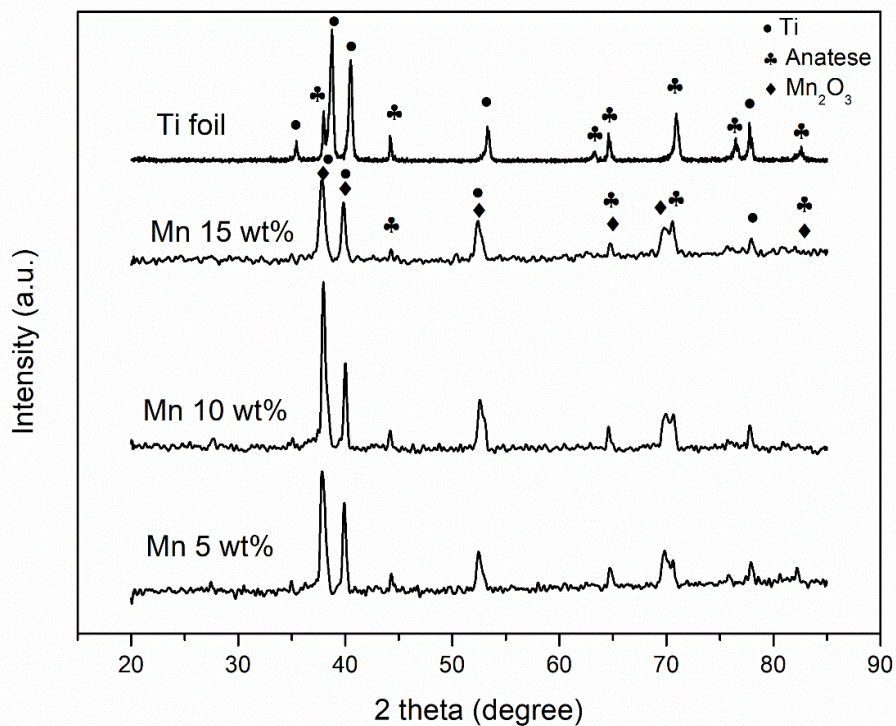
The XRD instrument was calibrated with silica powder from 28.3° to 28.6°. The data collected were then refined to determine the structure using X'pert High Score software. IR measurements of the samples were carried out with a Fourier transform infrared (FTIR) spectrometer (Perkin Elmer Spectrum 100) in the range of wave numbers of 4000 to 500 cm^{-1} . FESEM images were obtained using field emission scanning electron microscope equipped with an energy dispersive X-ray (EDX) (FESEM-EDX, JEOL JSM-7600F) to analyse the morphology of the surface and the elemental composition of the synthesised samples.

Evaluation of electrochemical properties

All electrochemical analyses have been carried out using a three-electrode cell system. Tests consisting of cyclic voltammetry tests (CV), galvanostatic charge-discharge testing (GCD) and electrochemical impedance spectroscopy (EIS) were carried out using the Autolab PGSTAT204/FRA32 M module, Metrohm. The counter, reference and working electrode were used as a platinum wire, an electrode Ag/AgCl (3 M KCl) and the prepared samples, respectively. The prepared carbon film MPC was measured with a potential range of -0.2 to 0.8 V. In order to test the capacitive and resistive behaviour of electrode/electrolyte interfaces, electrochemical impedance spectroscopy (EIS) test was performed. Parameters such as cell-electrolyte resistance (R_s) and charge transfer resistance (R_{ct}) can be obtained from Nyquist plots consisting of semicircles of high frequency and straight slopes of low frequency. In this study, EIS measurements were carried out between 0.01 and 1 000 000 Hz at a measured open circuit potential.

RESULTS AND DISCUSSION

Figure 1 shows X-ray diffractograms of synthesized $\text{Mn}_2\text{O}_3/\text{MPC}$ and different concentrations of Mn salt 5, 10 and 15 wt%, respectively. Although $\text{Mn}_2\text{O}_3/\text{MPC}$ is a thin film sample, Mn_2O_3 does not have a corresponding diffraction peak. EDX confirmed the presence of Mn_2O_3 based on the successful percentage of Mn deposited in carbon film MPC (Table 1). The main characteristics of the Mn_2O_3 phase [411] and [541] plane indexed to JCPDS No. 02-0902 are attributed to a small peak of about $2\theta \sim 40.80^\circ$ and 64.18° , respectively. Another four peaks corresponding to Mn_2O_3 were observed at $2\theta \sim 38.27^\circ$, 53.55° , 70.7° and 83.22° respectively, which also overlap with peaks of diffraction of Ti substrates. However, the appeared peaks slightly shifted (± 0.05) from the peaks of X-ray diffraction. The figure also proved that the structure remained unchanged in accordance with the XRD patterns due to the unchanged intensity of the peaks showing the crystalline phase even after manipulating different concentrations of Mn salt. It also indicated the crystal water dehydration did not damage the structure [25].



(a)

Figure 1: XRD patterns of composite film $\text{Mn}_2\text{O}_3/\text{MPC}$ at different concentrations vs Ti foil as substrate

Figure 2(a) and 2(b) depict the FESEM images of MPC and optimized composite film samples of $\text{Mn}_2\text{O}_3/\text{MPC}$ at 10 wt% of manganese salt, respectively. Figure 2(a) of MPC

sample shows a clear stripe pattern covering most of the surface with few open pores while Figure 2(b) depicts the manganese salt deposited as Mn_2O_3 nanoparticles on the MPC surfaces after the calcination.

The EDX analysis of the $\text{Mn}_2\text{O}_3/\text{MPC}$ composite film samples in Figure 2(c) shows that the key composite elements are C, Mn, Ti and O. It can be seen that Mn exist on the MPC surface in the form of Mn_2O_3 which are in accordance to the XRD results. When 10 wt% of Mn salt was added, the content of Mn_2O_3 in the $\text{Mn}_2\text{O}_3/\text{MPC}$ composite film was calculated to be 21.92 wt%. The dispersed Mn_2O_3 nanoparticles on the MPC surface can provide large Faradaic redox pseudocapacitance since the MPC can both significantly improve the electronic conductivity and provide double layer electrical capacitance. Therefore, it is anticipated that the composite film $\text{Mn}_2\text{O}_3/\text{MPC}$ will provide better supercapacitance than the pure MPC [4].

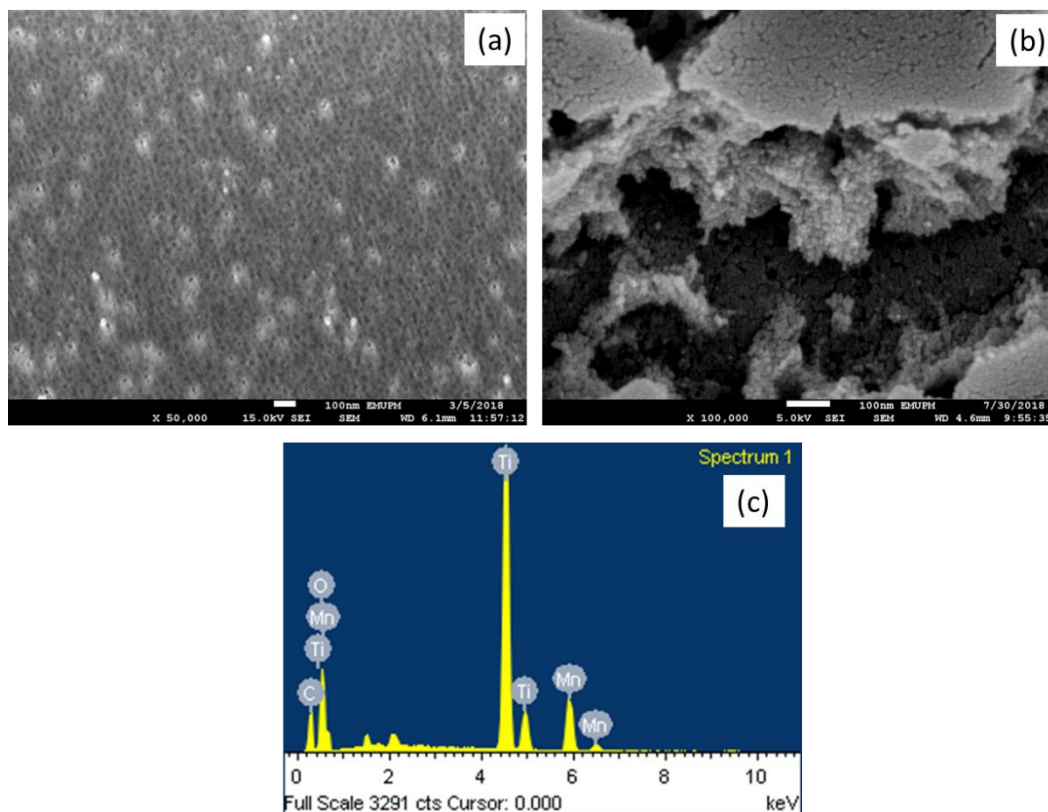


Figure 2: FESEM images of MPC (a) $\text{Mn}_2\text{O}_3/\text{MPC}$ composite film samples with 10 wt% manganese salt (c) EDX of $\text{Mn}_2\text{O}_3/\text{MPC}$ with 10 wt% manganese salt

Cyclic voltammetry was used to determine the electrochemical properties of the $\text{Mn}_2\text{O}_3/\text{MPC}$ composite film with different concentrations of Mn salt ranging from 0, 5, 10 and 15 wt%. Figure 3 shows the typical pseudocapacitive behaviour of the $\text{Mn}_2\text{O}_3/\text{MPC}$ electrodes. The calcined samples with 10 wt% of Mn content shows the

highest current response, indicating the highest electrochemical activity and the highest specific capacitance of 53.59 mF cm^{-2} as compared with the values of 15.23, 20.10 and 30.24 mF cm^{-2} for the samples calcined at 0 wt%, 5 wt% and 15 wt%, respectively. The CV curves for the composite electrodes showed significant redox peaks, indicating that there were faradic reactions during the charge-discharge process. The composite materials of manganese oxide-carbon had a combination of EDLC and pseudocapacitance which improved the overall performance by enhancing the specific capacitance.

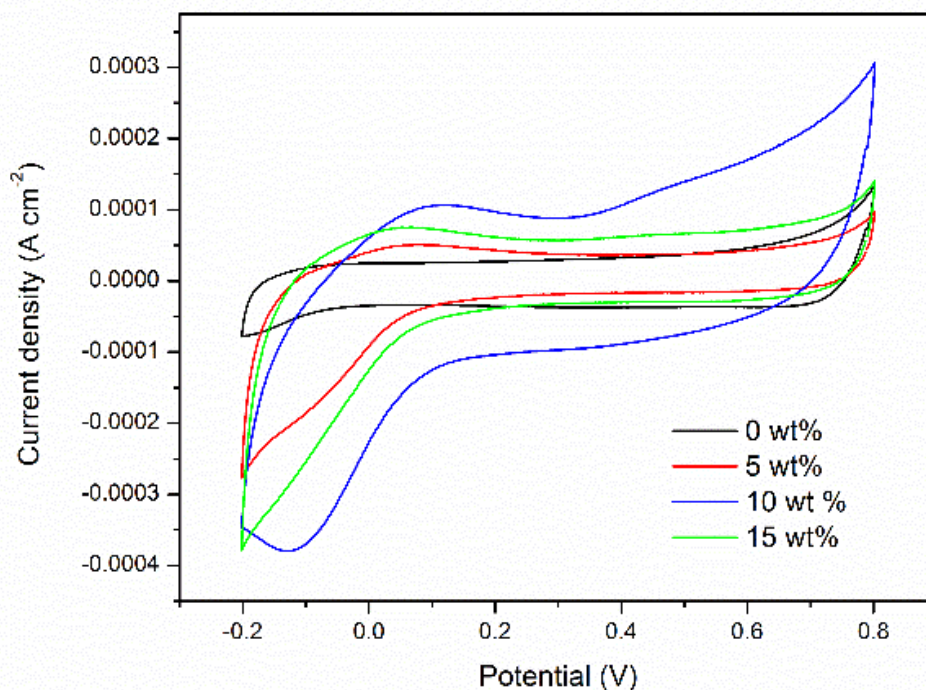


Figure 3: CV at different Mn salt concentration 0, 5, 10 and 15 wt% (See online version for colours)

Further analysis was carried out on the electrochemical performance using galvanostatic charge-discharge (GCD) curve. Figures 4 shows the GCD curves at different concentrations of Mn salt at the lowest current density of $400 \mu\text{A cm}^{-2}$ in 1 M KCl. It was observed that all samples showed charging and discharging curve. The specific capacitance calculated was 12.96 mF cm^{-2} , 23.14 mF cm^{-2} and 17.13 mF cm^{-2} at 5 wt%, 10 wt% and 15 wt%, respectively. The sample with longer charge/discharge time implies its higher electrochemical activity and specific capacitance than the samples with shorter charge/discharge time [23-24]. As the concentration of Mn salt increased, the specific capacitance decreased. At optimal Mn salt concentration, the improved uniformity and larger pores of the $\text{Mn}_2\text{O}_3/\text{MPC}$ composite film could provide better pathways for the electrolytes to flow through. This eventually led to a longer discharge time and higher specific capacitance of the composite sample [23].

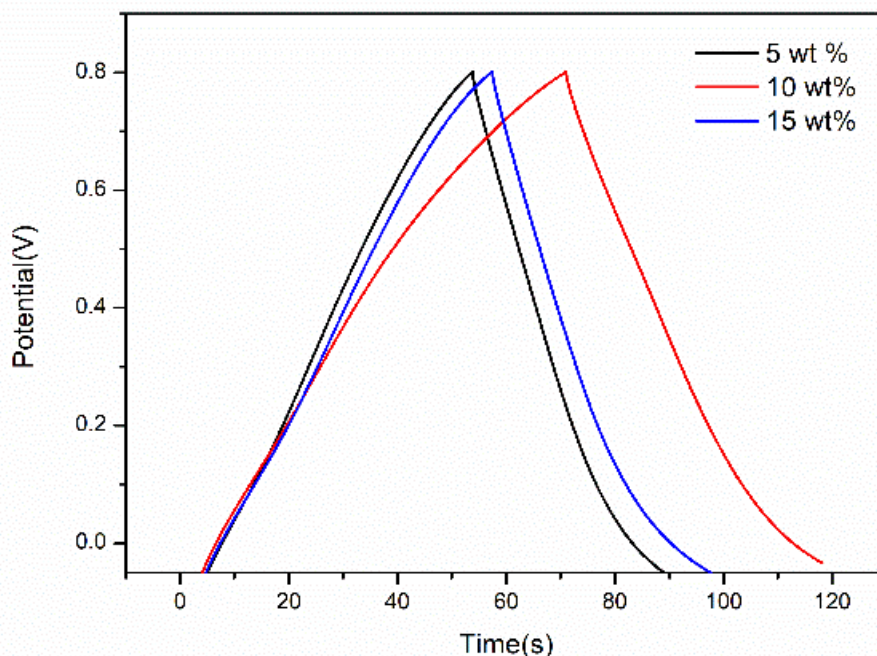


Figure 4: GCD at different Mn salt concentration 5, 10 and 15 wt% at lowest current density of $400 \mu\text{A cm}^{-2}$ (See online version for colours)

The electrochemical frequency for resistivity measurements on the equivalent series resistance (ESR) and resistance to charge transfer (R_{ct}) can be defined by the diameter of the formed semicircle of the electrode spectroscopy of the electrochemical impedance (EIS). The measurements were carried out in order to better understand the resistance behaviour of the synthesised samples. Values of resistance of the cell-electrolyte (R_s) and R_{ct} were determined using electrochemical circle fit (Table 1). The R_s and R_{ct} values for the optimum composite film $\text{Mn}_2\text{O}_3/\text{MPC}$ -10 wt% were 2.4Ω and 0.3Ω lower than MPC's carbon transfer resistance 2.6Ω and 0.4Ω , respectively. This impressive result of low internal resistance value for the composite samples could lead to the interpretation of higher specific capacitance depending on the results of the CV and GCD. Figure 5 shows clearly the Nyquist plots for MPC and $\text{Mn}_2\text{O}_3/\text{MPC}$ composite film. At the first intercepting point of the x-axis, the R_s or ESR values were detected and comprised the total resistance of the electrolyte and electrode in the lower part of the plot corresponding to the high frequency region. On the other hand, R_{ct} showed the charge transfer rate at the electrode and electrolyte interface, which was further influenced by the Faradaic redox process. The nearly linear vertical line across the x-axis of the higher resistivity region implied an almost ideal capacitive behaviour of the nanocomposite, and the steeper curving line indicated the rapid diffusion of the electrolyte ions [25].

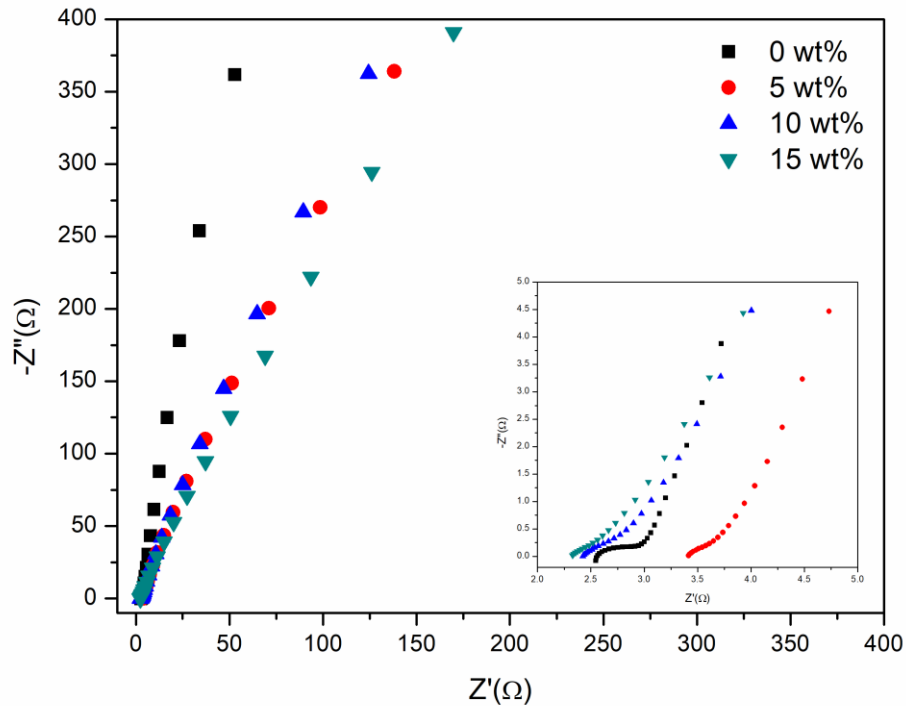


Figure 5: Nyquist plot for $\text{Mn}_2\text{O}_3/\text{MPC}$ composite film at Mn salt concentration of 0, 5, 10 and 15 wt%. Inset demonstrates the magnified version of the plot

Table 1: Cell-electrolyte resistance (R_s), charge transfer resistance and diameter semicircle (R_{ct}) of $\text{Mn}_2\text{O}_3/\text{MPC}$ at different concentration of Mn salt 0, 5, 10 and 15 wt% obtained from impedance analysis

Samples (wt%)	Cell electrolyte resistance, R_s (Ω)	Charge transfer, R_{ct} (Ω)
MPC-0 wt%	2.6	0.4
$\text{Mn}_2\text{O}_3/\text{MPC}$ -5 wt%	3.4	0.3
$\text{Mn}_2\text{O}_3/\text{MPC}$ -10 wt%	2.4	0.3
$\text{Mn}_2\text{O}_3/\text{MPC}$ -15wt%	2.3	0.4

CONCLUSIONS

The $\text{Mn}_2\text{O}_3/\text{MPC}$ composite film with different Mn content was successfully synthesised using a simple incipient wetness impregnation method followed by calcination to improve the supercapacitive behaviour of the composites. It was impregnated with the MPC film purposely to combine the excellent electrochemical

performance of mesoporous carbon film MPC with manganese oxide pseudocapacitive properties. For the optimal sample of 10 wt% Mn in the composite, the specific capacitance was 53.59 mF cm^{-2} . Due to the excellent electrical properties of the MPC carbon film and the faradaic redox reactions of Mn_2O_3 , the specific capacitance increased for the optimum sample. The R_s and R_{ct} values for the optimum composite film $\text{Mn}_2\text{O}_3/\text{MPC}$ -10 wt% were 2.4Ω and 0.3Ω lower than MPC's carbon transfer resistance, respectively. Therefore, incorporation of metal oxides in the $\text{Mn}_2\text{O}_3/\text{MPC}$ composite film is an effective way to increase the electrochemical performance in terms of specific capacitance characteristics of carbon materials for supercapacitor application.

ACKNOWLEDGMENTS

Universiti Putra Malaysia (UPM) supported this work under grant no.: GP/IPS/2017/9548000. JPA scholarship is gratefully recognized for the doctoral program for Mahanim Sarif @ Mohd Ali.

REFERENCES

- [1] Li, Y.H., Li, Q.Y., Wang, H.Q., Huang, Y.G., Zhang, X.H., Wu, Q., Gao, H.Q. and Yang, J.H. *Appl. Energy*. **153**, 78–86. (2015)
- [2] Zhang, Y., Xuan, H., Xu, Y., Guo, B., Li, H., Kang, L., Han, P., Wang, D. and Du, Y. *Electrochim. Acta*. **206**, 278–290. (2016).
- [3] Lokhande, V.C., Lokhande, A.C., Lokhande, C.D., Hyeok, J. and Ji, T. *J. Alloys Compd*. **682**, 381–403. (2016).
- [4] Wang, X., Liu, L., Wang, X., Yi, L., Hu, C. and Zhang, X. *Mater. Sci. Eng. B*. **176**, 15, 1232–1238. (2011)
- [5] Xia, H., Meng, Y.S., Yuan, G., Cui, C. and Lu, L. *Electrochem. Solid-State Lett*. **15**, 4, A60–A63 (2012)
- [6] Wang, H., Yi, H., Chen, X. and Wang, X. *Electrochim. Acta*. **105**, 353–361. (2013)
- [7] Meher, S.K. and Rao, G.R. *J. Phys. Chem. C*. **115**, (51) 25543–25556. (2011)
- [8] Chen, J., Huang, K. and Liu, S. *Electrochim. Acta*. **55**, (1) 1–5. (2009)
- [9] Zhang, Y., Li, G.Y., Lv, Y., Wang, L.Z., Zhang, A.Q., Song, Y.H. and Huang, B.L. *Int. J. Hydrogen Energy*. **36**, (18) 11760–11766 (2011)
- [10] Song, M.K., Cheng, S., Chen, H., Qin, W., Nam, K.W., Xu, S., Yang, X.Q., Bongiorno, A., Lee, J., Bai, J. and Tyson, T.A. *Nano letters*. **12**, (7) 3483-3490. (2012)
- [11] Yang, J., Yang, X., Zhong, Y.L. and Ying, J.Y. *Nano Energy*. **13**, 702–708. (2015)
- [12] Li, L., Wei, T., Wang, W. and Zhao, X.S. *Microporous Mesoporous Mater*. **123**, 1–3, 260–267. (2009)
- [13] Lee, Y. J., Park, H.W., Park, S. and Song, I. K. *CAP*. **12**, (1) 23–237 (2012)
- [14] Hu, C.C., Liu, M.J. and Chang, K.H. *Electrochimica Acta*. **53**(6), 2679-2687. (2008)

- [15] Gujar, T.P., Kim, W.Y., Puspitasari, I., Jung, K.D. and Joo, O.S. *Int. J. Electrochem. Sci.* **2**, 666-673. (2007)
- [16] Li, G.R., Feng, Z.P., Ou, Y.N., Wu, D., Fu, R. and Tong, Y.X. *Langmuir*. **26**, 4, 2209-2213. (2010).
- [17] Jiang, H., Yang, L., Li, C., Yan, C., Lee, P.S. and Ma, J. *Energy & Environmental Science*. **4**, (5) 1813-1819. (2011)
- [18] Wang, T., Peng, Z., Wang, Y., Tang, J. and Zheng, G. *Scientific reports*. **3**, 2693. (2013)
- [19] Mitome, T., Hirota, Y., Uchida, Y. and Nishiyama, N. *Colloids and Surfaces A: Physicochemical and Engineering Aspects*. **494**, 180-185 (2016)
- [20] Wang, Q., Zhang, W., Mu, Y., Zhong, L., Meng, Y. and Sun, Y. *Microporous and Mesoporous Materials*. **197**, 109-115. (2014)
- [21] Fisher, R.A., Watt, M.R. and Ready, W.J. *ECS Journal of Solid-State Science and Technology*. **2**, 10, M3170-M3177. (2013)
- [22] Mitome, T., Uchida, Y., Egashira, Y. and Nishiyama, N. *Colloids and Surfaces A: Physicochemical and Engineering Aspects*. **449**, 51-56. (2014)
- [23] Li, H., Zhang, X., Ding, R., Qi, L. and Wang, H. *Electrochimica Acta*. **108**, 497-505. (2013)
- [24] Poon, R., Zhao, X., Ata, M.S., Clifford, A. and Zhitomirsky, I. *Ceramics International*. **43**, (11) 8314-8320. (2017)
- [25] Wang, Y.T., Lu, A.H. and Li, W.C. *Microporous and Mesoporous Materials*. **153**, 247-253 (2012)